American Journal of Mechanical Engineering, 2015, Vol. 3, No. 2, 41-46
Available online at http://pubs.sciepub.com/ajme/3/2/2

DOI:10.12691/ajme-3-2-2

Hydro-Structure Analysis of Composite Marine Propeller under Pressure Hydrodynamic Loading

Hassan Ghassemi*, Manouchehr Fadavie, Daniel Nematy

Department of Ocean Engineering, Amirkabir University of Technology, Tehran, Iran
*Corresponding author: gasemi@aut.ac.ir

Received February 29, 2015; Revised April 04, 2015; Accepted April 13, 2015

Abstract This paper aims to predict the hydrodynamic characteristics and structural analysis of the marine propeller under pressure hydrodynamic loading. Because of the loading on the propeller blade, it goes under significant deformation that may affect the hydrodynamic performance of the propeller. Thus, the blade deformation of a propeller due to fluid pressure should be analyzed, considering hydro-elastic analysis. The propeller was made of anisotropic composite materials, and the geometry of the propeller is for one skew angle. First, the hydrodynamic pressure loading is obtained by FVM and then the deformation of the blade due to this pressure was calculated. Next, the pressure load for deformed propeller is achieved; it is again repeated to obtain the new deformed propeller. This procedure is repeated to converge the thrust, torque and efficiency. We present all results of the pressure distribution, hydrodynamic characteristics, stress and deformation of the propeller.

Keywords: *hydrodynamic characteristics, structural deformation, pressure and stress, composite material*

Cite This Article: Hassan Ghassemi, Manouchehr Fadavie, and Daniel Nematy, "Hydro-Structure Analysis of Composite Marine Propeller under Pressure Hydrodynamic Loading." *American Journal of Mechanical Engineering*, vol. 3, no. 2 (2015): 41-46. doi: 10.12691/ajme-3-2-2.

1. Introduction

Marine propellers are elements in which operate behind the vessel's hull and generate the desired thrust due to pressure loading on the blades. These propulsion systems are the most efficient driving equipment to drive the marine vessels. Meanwhile metal alloys were widely used from old days as conventional materials in manufacturing the propellers. Also, Nickel-Aluminum-Bronze and Manganese-Nickel-Aluminum-Bronze, because of their superior properties such as high strength, corrosion resisting and manufacturing, are alloys that mostly employed for propellers structure.

Nowadays composite materials applications are expanding in many industries such as aerospace, marines and many other vital vehicles. Composite materials have special properties such as light weight, strength-to-weight ratio, stiffens-to-weight ratio and easy manufacturing. Nowadays, extra enthusiasm for the use of composite materials in marine industries, in terms of improving properties and performance of structures, exists, especially in manufacturing the propeller blades as a result of anisotropic properties of these composite materials. Also, increase of efficiency and decrease of noise, fuel consumption, vibration, loading on blades, weight and pressure fluctuations are the common consequences of applying composite materials in marine propellers

According to increasing applications of composite materials, studying about these materials is needed more than ever. Due to complicated geometry of the propeller, structure analyzing is difficult. Many researchers have employed analytical and numerical method to determine the fluid-structure interactions of the propeller [1,2]. Formerly, cantilever beam theory is used for majority of investigations. Furthermore because of complicated shape of the blade FEM is mostly used for structural analyzing of propellers.

For hydrodynamic analysis and calculation of the pressure distribution on the propeller blade several methods have been developed until now; such as blade element theory, lifting lines theory, vortex lattice method and boundary element method. Lin and Lin worked on nonlinear hydro-elastic behavior of propellers using a finite-element method and lifting surface theory [3]. Cho and Lee [4] published an article entitled propeller blade shape optimization for efficiency improvement. They studied an optimization method to generate the optimal shape of the propeller to increase the efficiency. Meanwhile lifting line theory and lifting surface theory are applied for hydrodynamic calculations.

A coupled BEM-FEM method for exploring the fluid structure interaction of flexible composite marine propellers is developed by Young [5,6]. Also, Young and Motely investigated influence of material and loading effects on the propellers made of advanced materials [7]. Lin et al. published nonlinear hydroelastic behavior of propellers using a finite-element method and lifting surface theory [8] and also experimental paper which presented optimization and experiments on a composite propeller [9]. A FSI (fluid structure interaction) analysis for a flexible propeller is done by Sun et al. [10]. Kulczyk and Tabaczek studied the propeller-hull interaction in the

propulsion system [11]. The application of composite materials on the ships propeller performance is investigated by Takestani et al. [12]. Also, other works of the hydro-elastic analysis of marine propellers have been performed in [13,14].

The boundary element method (BEM) is widely used for analyzing the flow around the propellers. This method is applied in three-dimensional turbulence flow, based on potential theory. The BEM is developed for simulating the cavitation in face and back of the immersed, supercavitation and surface piercing propeller in wake flow by Kinnas and Fine [15]. Additionally, the accuracy of this method was so good for no vibration case, pressure and cavitation calculated by BEM was considerably close to experimental results. Ghassabzadeh and Ghassemi employed a hybrid BEM-FEM to determine the hydrodynamic characteristics of a composite propeller based on hydro-elastic analyzing [16]. Recently, investigation of different methods of noise reduction for submerged marine propeller s and their classification carried out by Feiz Chekab et al. [17].

In this paper, finite volume method is used to calculate the hydrodynamic pressure. On the other hand, the blade deformation is analyzed by FEM. Firstly, the hydrodynamic pressure for undeformed propeller is calculated by FVM and the results are exported to the FEM. Then the strain and stress of the blade is calculated. After that the pressure distribution on the propeller using the deformed shape of the blade is recalculated and the new pressure loading is exported to the FEM code and evaluate new deformation again. This process was repeated until the optimum shape and results are obtained.

2. FVM-FEM Coupled

The finite volume method with coupled finite element method employed to the present calculations. Pressure on the blade of the propeller and hydrodynamic characteristic of the propeller are first calculated by FVM. Deformed blades and stress results may be determined by finite element method.

Here, the computational results of thrust and torque compared to experimental results [16] for B-series propeller are shown in Figure 1, which examine a very good agreement between them. In other word, the numerical results based on experimental data were proved.

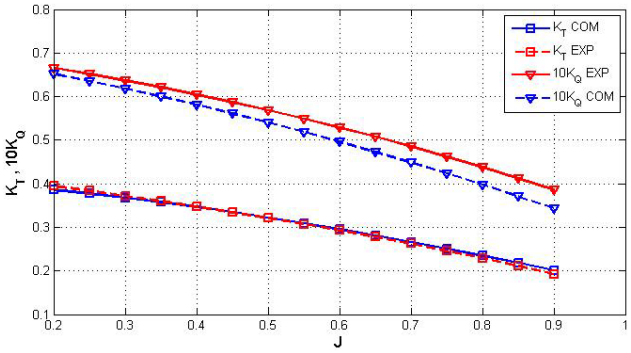

Figure 1. Comparison of computational and experimental hydrodynamic characteristic

Geometry and Computation Grid

In this paper, a marine propeller for B-series was chosen and modeled. The results of hydrodynamic and structural analyzing were presented. The process is according to the flowchart shown in Figure 2. The propeller geometric properties were also shown in Table 1, given from reference [16].

Table 1. Propeller Geometry Properties

parameter	Value
Number of Blades	5
Diameter	0.5 m
Hub Ratio	0.2
Pitch Ratio	Variable (at 0.7R=0.8)
Expanded Area Ratio (EAR)	0.65
Skew Angle	Variable (at 0.7R=25 degree)
Rake Angle	10 degree

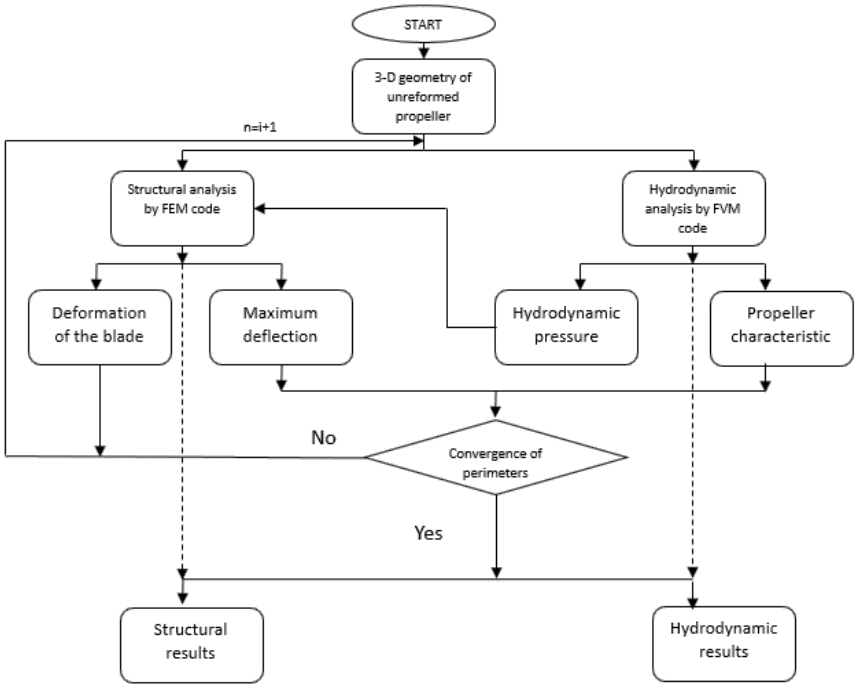

Figure 2. Calculations flowchart

At the beginning of the process, the propeller geometry and domain is generated as shown in Figure 3. The Cartesian coordinates system is used, where x,y and z denote downstream, starboard and upward direction respectively. The origin was located at the center of the hub, and positive directions are upstream, starboard and downstream. The domain dimensions were shown in Figure 4. The solution field was divided into global and sub-domain. The sub-domain frame simulates the propeller rotation and employs the Coriolis acceleration terms in the governing equations for the fluid. The global frame surrounds the sub-domain frame. The global frame is a circular cylinder with 4D diameter, where D is the propeller diameter. The distance between the sub-domain frame and inlet is nearly 4D, while it is nearly 6D for the outlet and dynamic frame. The sub-domain is sphere with a diameter of D.

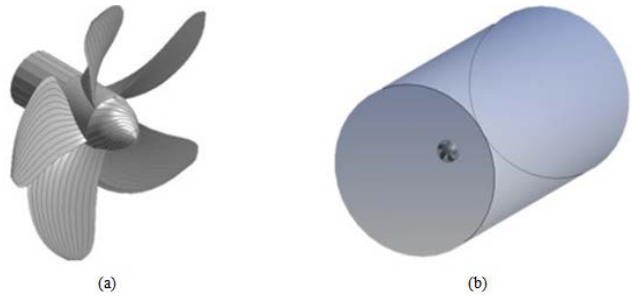

Figure 3. (a) 3D propeller (b) calculation domain

Discretized domain around propeller is illustrated in Figure 5. In the next step, boundary conditions are imposed. For this case we divided the solution field into two blocks. The rotating block was meshed with unstructured tetrahedral cells. These elements have a smaller size because the flow around the propeller blade is varying, and we need more accuracy there. The other block is meshed also with unstructured tetrahedral elements. In this block, the sizes of the elements are bigger because the flow in this region is smoother, and smaller grids just cause longer calculation procedure. We employed different grid number and it is concluded that with number of elements 991640 are sufficient for the present calculations.

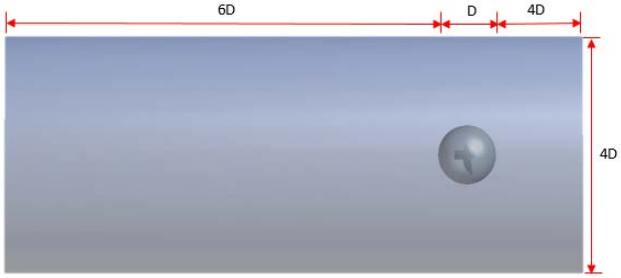

Figure 4. Domain dimensions

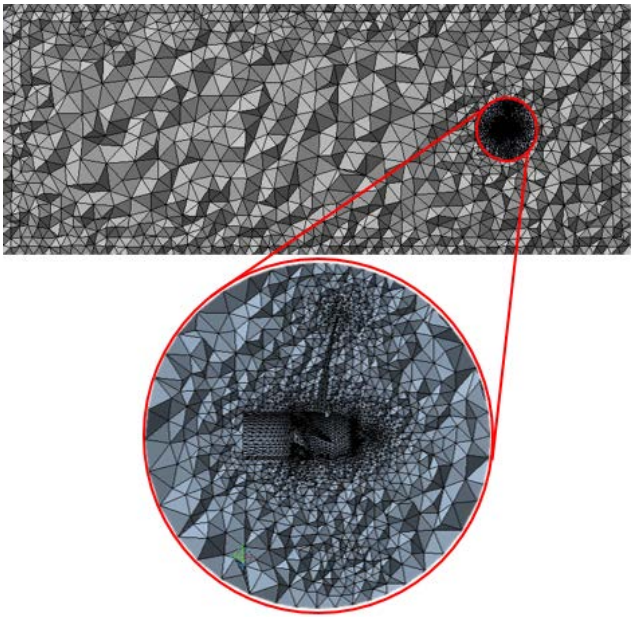

Figure 5. Domain descritization

Table 2. Mechanical Properties of Composite and Coper High Tensile Brase

Property Material	Modulus of elasticity (GPa)	Poisson ratio	Shear modulus elasticity (GPa)	Density (ton/m3)
Composite	E_x=132 E_y=10.8 E_z=10.8	v_{xy}=0.24 v_{yz}=0.49 v_{xz}=0.24	G_{xy}=5.65 G_{yz}=3.38 G_{xz}=5.65	ρ_P=1.5
Copper High Tensile Brass	E_z=102.97	v_{xz}=0.35	-	ρ_P=8.25

Boundary Conditions and Numerical Setups

In the present paper, we used CFX solver in order to evaluate the hydrodynamic performance of a B-series propeller. The governing equations of this problem were solved by the finite volume method based on the RANS equations. A SIMPLE algorithm was used for solving the pressure-velocity coupling equations. The k-epsilon model was used for turbulence model. The fluid (water) was assumed as an incompressible fluid, therefore; on the inlet boundary, uniform velocity is imposed and on the outlet boundary, pressure outlet was imposed. The axial velocity is 0.2m/s in the opposite direction. The no-slip wall condition was imposed on the propeller blades.

ANSYS structural 14 used for structural analyzing. The solver type was iterative. Propeller blade was made of linear elastic anisotropic composite with mechanical properties as shown in Table 2. We also define a fixed support at the end of the hub.

Hydrodynamic and Structural Results

The performance characteristics of the marine propeller can be defined using the non-dimensional coefficients such as the advance ratio, thrust coefficient, torque coefficient, and efficiency, which can be computed, respectively, as follows:

$$\begin{cases} J = \dfrac{V}{nD}, & K_T = \dfrac{T}{\rho n^2 D^4} \\ K_Q = \dfrac{Q}{\rho n^2 D^5}, & \eta = \dfrac{J}{2\pi}\dfrac{K_T}{K_Q} \end{cases} \quad (1)$$

After solving, the pressure contour, at J=0.2, in face and back of the deformed propeller is shown in Figure 6 and Figure 7, respectively. It is clear that the deformation of the blade affects the pressure distribution. The hydrodynamic pressure of the deformed blade is less than

that of the undeformed blade. As can be seen the pressure in regions near to the root has its maximum amount and as we move toward the tip the pressure loading, due to structural reasons, decreases. However, areas near to mid-sections, between 0.5R and 0.7R generate the most thrust.

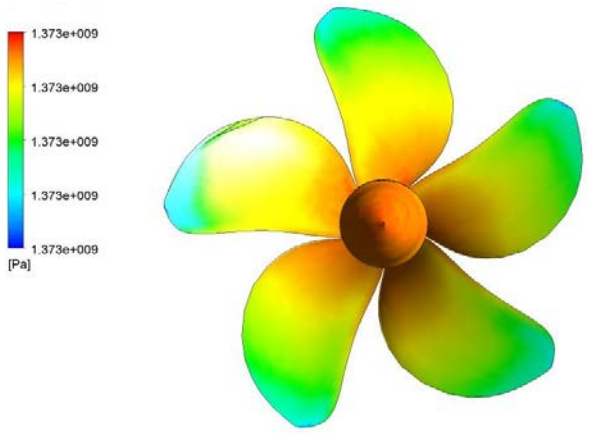

Figure 6. Pressure contour in face

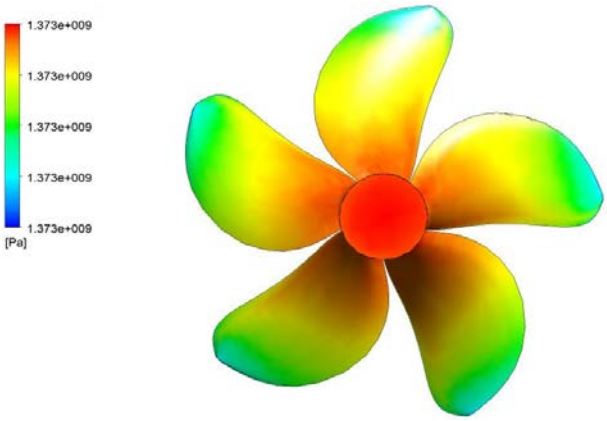

Figure 7. Pressure contour is back

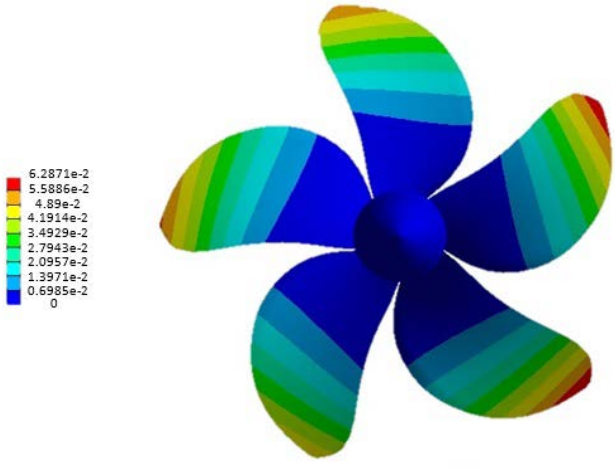

Figure 8. Deformation field of the propeller blade

Figure 8 shows the deflection of the blade along the radial at J=0.2. From the hydrodynamic point of view, applied loading on the blade is the heavy condition that may act to reach high deformation. As can be seen, deflections are distributed according to the nonlinear function. Blade is deformed higher at the tip. Maximum deflection is about 6 cm at the tip. The reason of this phenomenon is that a major thrust was generated in middle sections of the blade and also as we move toward the tip the bending moment about the root increases. Also, if deformation of the blade monitored carefully, the deformation of the trailing edge is more than of the leading edge. There is also an explanation for that, the stress, which illustrated in following Figures, is higher in the trailing edge.

The deformed and undeformed shape of the blade were shown with ten times enlargement at J=0.2, in Figure 9. As mentioned earlier, the deformation increases from root to tip of the blade, due to structural reasons mentioned earlier. The vectors of deformation or one blade is shown in Figure 10.

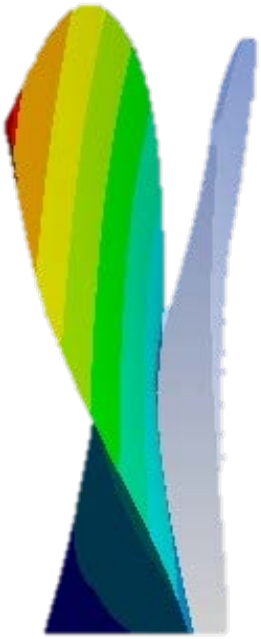

Figure 9. Deformed and undeformed blade of the propeller

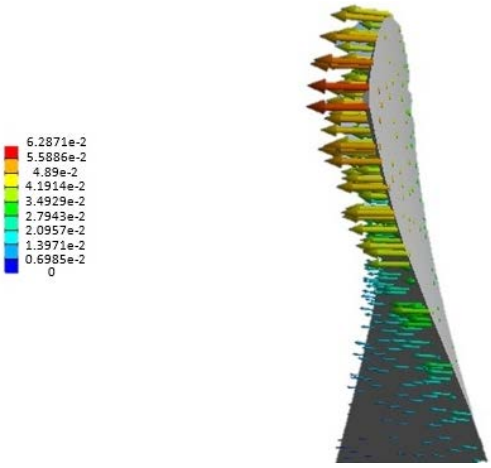

Figure 10. Deformation vectors of the blade

The equivalent von-misses stress in the face and back of the propeller was shown in Figs. 11 and 12 respectively. The stress in the trailing edge has its maximum value and as we move towards the other sections of the blade the equivalent stress decrease. The stress in tip is about 22% of maximum equivalent stress and in the leading edge in about 66.5% of maximum equivalent stress. In the back of the propeller in middle sections, we have the maximum equivalent stress and as we move to the other blade sections the stress decrease.

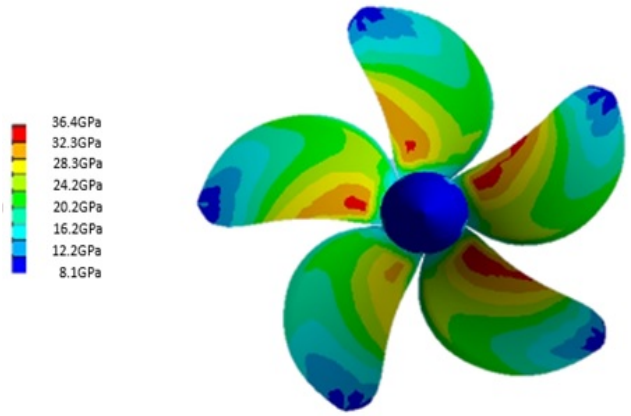

Figure 11. Equivalent stress in the face of the propeller

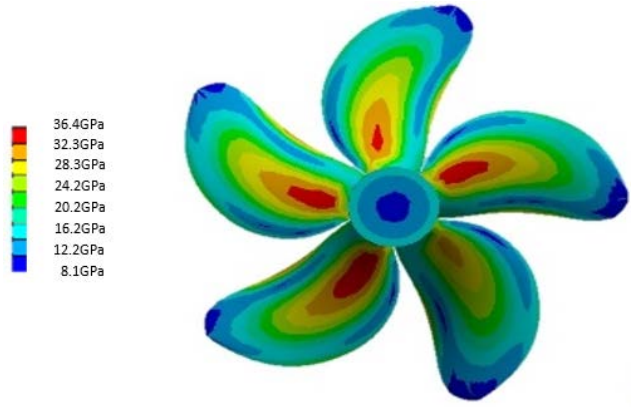

Figure 12. Equivalent stress in the back of the propeller

Figure 13 shows the maximum deflection versus the advanced velocity ratio; it is clear that, an increase in advanced velocity ratio causes the maximum deflection of the blade to decrease. Therefore, the maximum deflection for the propeller occurs at J=0.2.

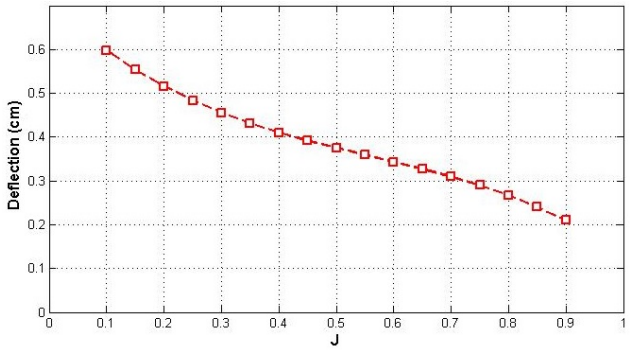

Figure 13. Deflection of the blade versus advanced coefficient

In Figure 14, the hydrodynamic coefficient of the propeller versus the advanced coefficient is presented for deformed and undeformed propellers. Deformed propeller gives lower efficiency relative to the undeformed propeller, especially at high advance ration.

In order to examine the effect of the advanced velocity ratio on the hydrodynamic characteristics precisely, the relative error of the propeller characteristics relative to those of the undeformed blade are shown in Figure 15 at all advanced velocity ratio. It is clear that relative error in the propeller characteristics are nearly constant, and so the performance of the propeller is independent of the rotational speed and the advance velocity.

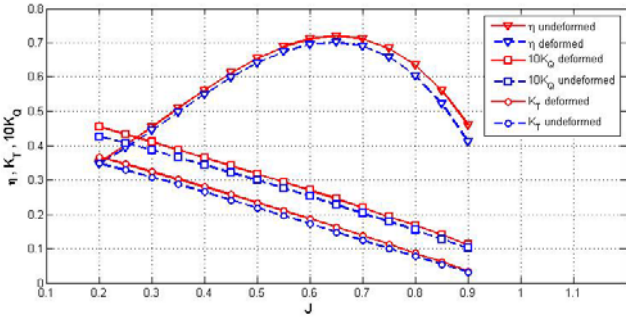

Figure 14. Hydrodynamic coefficients of deformed and undeformed propeller

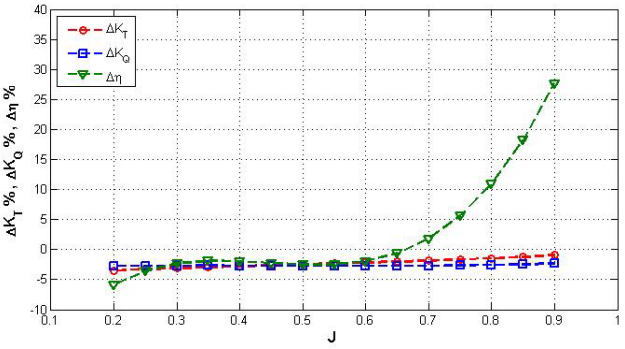

Figure 15. Relative error in hydrodynamic coefficients

3. Conclusions

In the present paper, coupled FVM-FEM hydro-elastic procedure was used to investigate the hydrodynamic and structure behavior of a marine propeller. The solving procedure was an iterative process; the hydrodynamic pressure was calculated in FVM code and the structural analysis performed by FEM code. In the case study, a five blade composite propeller was chosen to study the deformations and the effect of deformation on the propeller performance. Admittedly, the deformation toward the blade tip increases and stress decreases. The stress in the face of the blade and leading edge is maximum and in back and in the middle of the blade, and as moves to the other areas decrease. Increasing in advanced velocity ratio causes the maximum deflection, the thrust coefficient and the torque coefficient decreases.

We also determined the effect of this deformation on the propeller hydrodynamic performance. Obviously, in low advanced coefficients, when the propeller is working in heavy conditions, both thrust force coefficient and torque coefficient increase. While the propeller performance decrease. Hydrodynamic coefficients of the propeller are approximately constant. That means that the deformation of the propeller is independent of the advance velocity ratio.

Acknowledgment

This research was supported by the Marine Research Center (MRC) of Amirkabir University of Technology (AUT) whose works are greatly acknowledged.

References

[1] Blasques, J. P., Berggreen, C., and Andersen, P. (2010). Hydro-elastic analysis and optimization of a composite marine propelle. *Marine Structures, 23* (1), 22-38.

[2] Cho, J., and Lee, S.-C. (1998). Propeller Blade Shape Optimization for Efficiency Improvment. *Computers and Fluids, 27* (3), 407-419.

[3] Li, G., Li, W., You, Y., and Yang, C. (2013). Study on Fluid-Structure Interaction Characteristics of Composite Marine Propeller. *In The Twenty-third International Offshore and Polar Engineering Conference.* Anchorge: International Society of Offshore and Polar Engineers.

[4] Lee, H., Song, M. C., Suh, J. C., and Chang, B. J. (2014). Hydro-elastic analysis of marine propellers based on a BEM-FEM coupled FSI algorithm. *International Journal of Naval Architecture and Ocean Engineering, 6* (3), 562-577.

[5] Young, Y. L. (2007). Fluid–structure Interaction Analysis of Flexible Composite Marine Propellers. *Journal of fluids and structures.*

[6] Young, Y. L. (2006). Numerical and experimental investigations of composite marine propellers. *Proceedings of Twenty-Sixth Symposium on Naval Hydrodynamics.* Rome.

[7] Young, Y. L., and Motley, M. R. (2011). Influence of Material and Loading Uncertainties on the Hydroelastic Performance of Advanced Material Propellers. *Second International Symposium on Marine Propulsors*, (pp. 10-17). Hamburg.

[8] Lin, H. J., and Lin, J. J. (1996). Nonlinear hydroelastic behavior of propellers using a finite-element method and lifting surface theory. *Journal of Marine Science and Technology, 1* (2), 114-124.

[9] Lin, C. C., Lee, Y. J., and Hung, C. S. (2009). Optimization and experiment of composite marine propellers. *Composite Structures, 89* (2), 206-215.

[10] Sun, H. T., and Xiong, Y. (2012). Fluid-structure interaction analysis of flexible marine propellers. *Applied Mechanics and Materials, 226* (228), 479-482.

[11] Kulczyk J. and Tabaczek T. (2014) Coefficients of Propeller-hull Interaction in Propulsion System of Inland aterway Vessels with Stern Tunnels, *the International Journal on Marine Navigation and Safety of Sea Transportation*, Vol. 8 No. 3.

[12] Takestani, T., Kimura, K., Ando, S., and Yamamoto, K. (2013). Study on Performance of a Ship Propeller Using a Composite Material. *3rd International Symposium on Marine Propulsors.* Launceston, Tasmania.

[13] He, X. D., Hong, Y., and Wang, R. G. (2012). Hydroelastic optimisation of a composite marine propeller in a non-uniform wake. *Ocean Engineering, 39*, 14-21.

[14] Mulcahy, N. L., Prusty, B. G., and Gardiner, C. P. (2010). Hydroelastic tailoring of flexible composite propellers. *Ships and Offshore Structures, 5* (4), 359-370.

[15] Kinnas, S. A., and Fine, N. E. (1993). A Boundary Element Method for the Analysis of the Flow Around 3-d Cavitating Hydrofoils. *Journal of Ship Research, 3* (37), 213-224.

[16] Ghassabzadeh, M., Ghassemi, H., and Saryazdi, M. G. (2013). Detrmination of Hydrodynamics Characteristics of Marine Propeller Using Hydroelastic Analysis. *Brodogradnja, 64* (1), 40-45.

[17] Feizi Chekab M., Ghadimi P., Djeddi, S.R., Soroushan M., Investigation of Different Methods of Noise Reduction for Submerged Marine propeller s and Their Classification, *American Journal of Mechanical Engineering*. 2013 1 (2).